Software Tools for Visualizing Multivalued Functions

Gabriel Katz

Massachusetts Institute of Technology

Cambridge, MA 02139, USA

gabkatz@gmail.com

Vladimir Nodelman

Holon Institute of Technology

Holon, 52 Golomb St., 58102, Israel

nodelman@hit.ac.il

Abstract.

The existing Computer Algebra Systems (like "MathLab", "Mathematica", and similar applications) are designed for professional mathematicians and engineers. They do not support at all, or only partially support dynamical interactions with graphical models. In any case, these tools require some mastery of nontrivial and cumbersome programming syntax (for example, see Mathematica [11]— an obvious obstacle for the inexperienced learners of mathematics. The uniform non-formulaic interface for manipulating with virtual graphical models is lacking in the traditional Computer Algebra Systems. On the other hand, the popular dynamic geometry applications (like "Geometer's SketchPad"[5] or "Cinderella"[3]) are limited by their 2D-nature.

"VisuMatica", a comprehensive software package for visualizing and investigating mathematics, is designed to fill in this educational niche.

In the paper, we aim to show how VisuMatica can handle virtual experiments in the intricate universe of multi-valued functions. Difficulties in grasping the concept of multivalued functions partially are due to the lack of adequate tools for their visualization. We present templates of visual models and interactive activities that could help students to explore the universe of multi-valued functions and to study the topology of Riemann surfaces.

Multivalued functions, software, visualization.

The Challenge of Multi-valued Arithmetics

Perhaps, in the first time students meet with the concept of multivalued functions when dealing with the quadratic formula. The second encounter with the idea occurs in high school, while studying the notion of roots of complex numbers. This subject becomes especially important in the algebra of polynomial equations and in the complex analysis.

Life in the world of multi-valued functions is hard: even adding them is a questionable operation! Just think how would you interpret, say, the formula $\sqrt{2+3i} + \sqrt{1-i}$? Does it represent *four* complex numbers—all the possible sums of a number from the

two-element set $\sqrt{2+3i}$ and a number from the two-element set $\sqrt{1-i}$? If so, how about the product $\sqrt{2+3i} * \sqrt{1-i}$? That set must consist only of two elements because $(\pm 1)*(\pm 1)$ = $(\pm 1)*(\mp 1) = (\pm 1)$! Along the same lines, is it true that $\sqrt{z} + \sqrt{z} = 2\sqrt{z}$? Well, if $\sqrt{z}$ takes two values, say a and $-a$, then the possibilities for $\sqrt{z} + \sqrt{z}$ are: $2a$, $-2a$, and $0 = a + (-a)$. On the other hand, the possibilities for $2\sqrt{z}$ are only $2a$ and $-2a$.

So the standard algebraic rules for operating with regular functions fail miserably when dealing with multi-valued ones.

Domain-Range Visual Representations of Multi-valued Functions

In order to visualize a map f: $\mathbf{C} \rightarrow \mathbf{C}$ of complex planes on a computer screen, we separate the domain and range of f and show them in two different views-windows [9]. This presentation helps to visualize the correspondence between the source z and the target(s) $f(z)$. For example, we can use the colour coding to indicate the correspondence (compare this interface with [4], [10] and [12], where only the range window is available).

Let us start with the example of how *VisuMatica* represents the multi-valued function $f(z)$ = $\sqrt[5]{z}$ (it describes all the solutions of the complex equation $w^5 = z$ for a variety of complex numbers z) (see Fig. 1). As we move the cursor over the point z of the complex plane (the domain window), the set of values $\sqrt[5]{z}$ is displayed in a different complex plane (the range window). The color-coding emphasizes the five-fold ambiguity in determining the value of f in the range. Note that the five images of z share their colour with z (currently yellow).
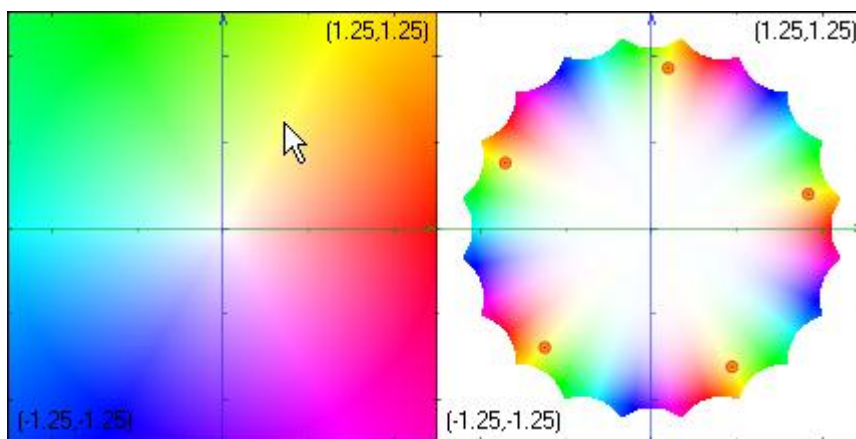

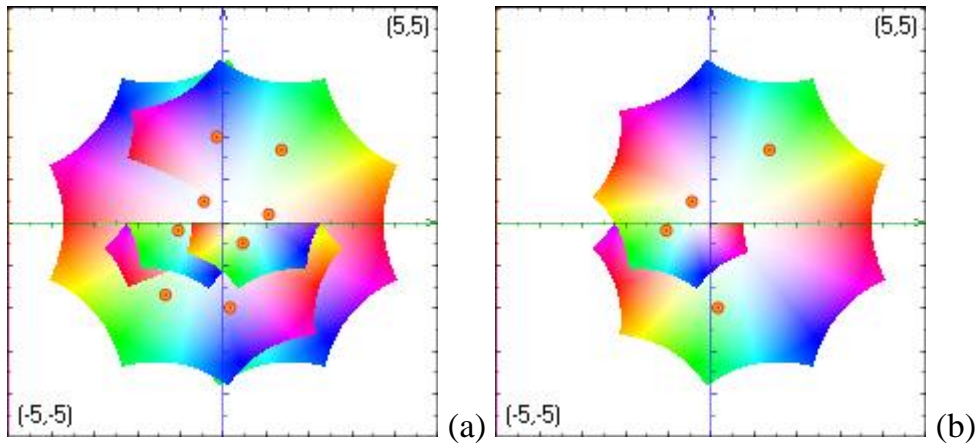Figure 1. The multi-valued image of the cursor under the map $z \rightarrow \sqrt[5]{z}$

Figure 2. The range view of the function $w = \sqrt{z} + \sqrt{0.1 + \sqrt{z}}$

(the cursor resides at $z = -1 + i$):

a) the disabled (default) option "*eliminate multi-valued repetitions*" produces 8 values,

b) the enabled one produces only 4 values by treating the two occurrences of $\sqrt{z}$ as equal.

Occasionally, a dynamic visualization of multiple values of a function becomes difficult if done by moving the mouse manually. In such cases, we can specify the mouse trajectory analytically. For example, consider the 6-valued function $f(z) = \sqrt[3]{-\dfrac{z-i}{2} + \sqrt{\dfrac{(z-i)^2}{4} + \dfrac{z^3}{27}}}$. The task is to see the trajectories traced by its multiple values, as the pointer at z moves, say along the circle of radius 1.25, centred on the origin. Fig. 3 shows the image trajectories.

Using the "Simulation" tool of the "Mapping" dialog box and moving the slider (marked by an arrow in Fig. 3), the user can control the movement of z in the domain and of its image(s) $f(z)$ in the range. The value of the polar coordinate of z is automatically updated in the textbox on the right side of the slider. One can type in this textbox the value of an angle; the pointer and its corresponding six images (the small red circles) will appear in the Range window.
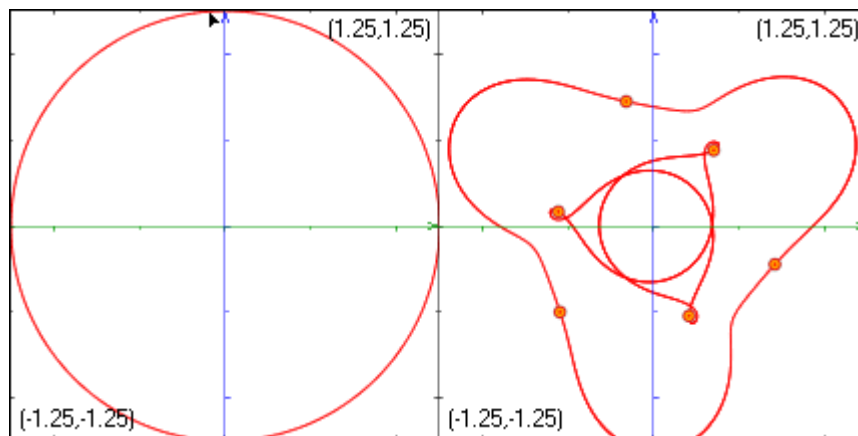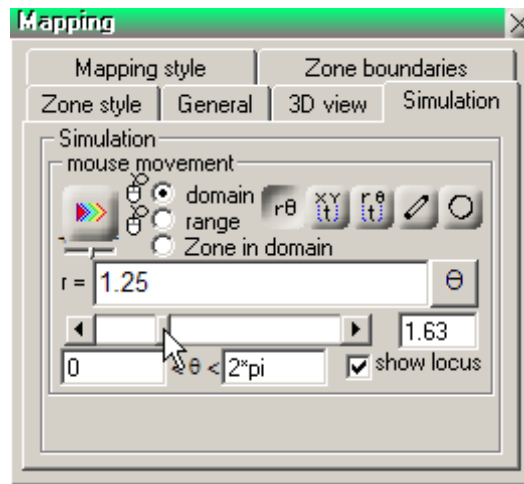
Figure 3. The 6 images of the cursor on the circle trace two loops; each loop contains 3 images of the cursor, controlled by the "Simulation" tool of "Mapping" dialog box.

Multi-valued Functions and Riemann Surfaces

Problems with the arithmetic of multi-valued functions have an elegant solution. In the case of multi-valued *analytic* functions of a single complex variable, the proposed solution is called "*The Riemann Surface*". On technical level, the construction of Riemann surfaces is based on the principle of analytic continuation. However, here we adopt a more geometrical viewpoint. In any case, our goal here is not to introduce the reader to the classical theory of Riemann surfaces (see [2], [8]), but to show the usefulness of VisuMatica in generating expressive dynamic images, the images that facilitate our understanding of the subject.

At the first glance, the idea of a Riemann surface looks as a cheap trick: we replace the domain of a given multi-valued function by a new more complex domain on which the function becomes *single-valued*.

Let us illustrate this trick with the simplest possible example. Take the 2-valued function $f(z) = \sqrt{z}$ of the complex variable z. Consider the complex algebraic curve (the real surface) Σ in $\mathbf{C}^2$ whose equation is $\{w^2 = z\}$, a complex parabola. If $w = u + iv$ and $z = x + iy$, then, in the real $uvxy$-space, Σ can be also described by two quadratic polynomial equations: $\{x = u^2 - v^2, y = 2uv\}$.

As we try to express w in terms of z, we get $w = \sqrt{z}$, our original 2-valued function.

Now replace $\mathbf{C}$, the domain of $\sqrt{z}$, with the curve/surface Σ, and $f(z) = \sqrt{z}$ with the coordinate w, viewed as a *single*-valued function on Σ. Note that the coordinate w is a map from $\mathbf{C}^2$ to $\mathbf{C}$ and thus can be applied to any subset in its domain, including the complex curve Σ. This complex curve Σ, equipped with the coordinate maps $z: \Sigma \to \mathbf{C}$ and $w: \Sigma \to \mathbf{C}$, *is* the Riemann surface of the function $\sqrt{z}$.

So how can we visualize this and other Riemann surfaces? Since we do not have the gift of seeing a 2-dimensional object in a 4D-space, we need to downgrade our ambitions to 2-dimensional objects in 3D. Here is where *VisuMatica* becomes handy. Of course, such a 3-dimensional picture will not give a faithful representation of the way Σ resides in $\mathbf{C}^2$. Nevertheless, it will be very useful for understanding the geometry of Σ in connection to both coordinates z and w in $\mathbf{C}^2$. Moreover, an appropriate *pair* of such 3D-images will constitute a *faithful* representation of Σ in $\mathbf{C}^2$.

Let us examine a more general setting. Let $G(z, w)$ be a complex polynomial of degree d in the variables z and w. Consider an algebraic curve (a real surface) Σ whose equation in $\mathbf{C}^2$ is $G(z, w) = 0$. How is it possible to draw Σ ?

Here is the main idea behind traditional depictions of Σ in 3D. Let F_a stand for the intersection of Σ with the complex line $\{z = a\}$. If a polynomial $G(z, w)$ of degree d is not divisible by $(z - a)$, then F_a is a finite set of cardinality d at most. Consider $w(F_a)$, the w-image of F_a in $\mathbf{C}$. Pick one of the following standard coordinate functions $x: \mathbf{C} \to \mathbf{R}$ or $y: \mathbf{C} \to \mathbf{R}$ (as usually, $x(z) = \mathsf{Re}(z)$ and $y(z) = \mathsf{Im}(z)$). For each z in $\mathbf{C}$, apply the function x (or y) to the set $w(F_z)$ in $\mathbf{C}$ to produce the set $x(w(F_z))$ in $\mathbf{R}$. Let V be the real 3D-space of pairs (z, t), where z is a complex number and t is a real number. Consider a surface Σ_x in V, formed by the pairs (z, t), where z runs over $\mathbf{C}$ and t belongs to the finite set $x(w(F_z))$ "suspended over z". Similarly, employing the function $y: \mathbf{C} \to \mathbf{R}$, we can construct another surface Σ_y in V. We view both surfaces, Σ_x and Σ_y, as representing the same Riemann surface Σ. Each of them gives a lot of information about Σ; together they form its faithful representation.

Riemann surfaces Σ have an interesting *topology*. It can be recovered from their images (like Σ_x) in 3D. For a *generic* degree d polynomial $G(z, w)$, *topologically* Σ is a 2-sphere to which $(d - 1)(d - 2)/2$ handles have been attached and from which d points have been deleted (see the left picture in Fig. 4). In particular, for $d = 2$, we get a 2-sphere with two punctures; for $d = 3$, we get a torus (the surface of a bagel) with three punctures. When Σ has singularities (for example, simple self-intersections), its topology is more complex (see the right picture in Fig. 4). In such a case, Σ can have singularities that are obtained by identifying a number of points on a punctured 2-sphere with $(d - 1)(d - 2)/2$ handles into a single point. For example, in the vicinity of a simple self-intersection point, Σ looks like a double cone (consider the vicinity of bold black points in Fig.4).
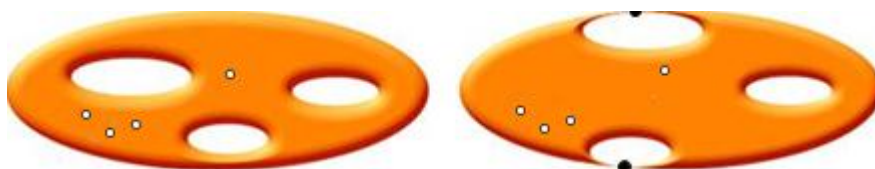

Figure 4. Some topological types of Riemann surfaces

Fig. 5 shows the surface Σ_x for the familiar quadratic parabola $\Sigma = \{z - w^2 = 0\}$, the Riemann surface of the multi-valued function $z^{\{1/2\}}$. Even in this most basic case, reconstructing the topological type of Σ from these pictures takes some thought. In fact, Σ is a 2-disk, or a 2-sphere with a single puncture.

Often it is more expressive and informative to show the intersections of the surfaces Σ_x or Σ_y with the surface of a square prism $\{|\mathsf{Re}(z)| \leq r, |\mathsf{Im}(z)| \leq r\}$ (see Fig. 5, (a) and (b)) or with the surface of a circular cylinder $\{|z| \leq r\}$ (see Fig. 5 (c) and (d)), both residing in the 3D-space $V = \mathbf{C}^1{}_z \times \mathbf{R}^1{}_t$.

In Fig. 5, (b), the intersections of Σ_x with the *surface* of ~~the~~ prism is shown as a narrow self-intersecting colourful band, while the intersections of Σ_x with the prism itself look semitransparent.
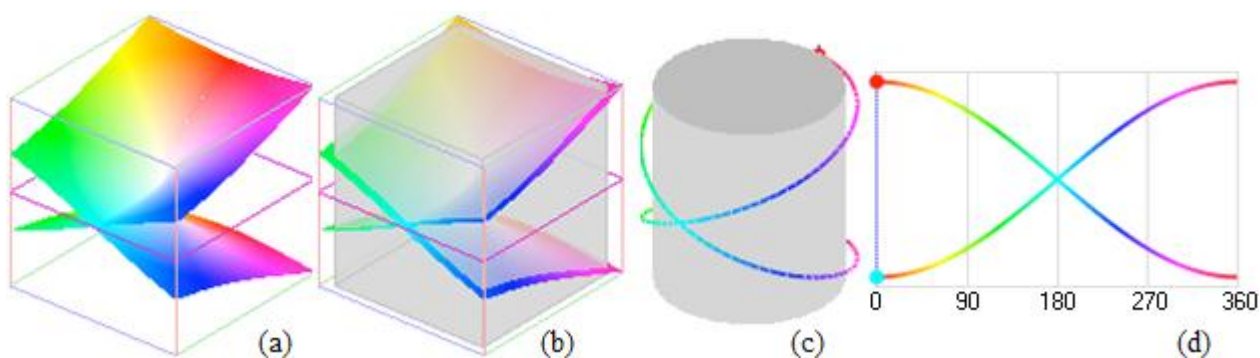

Figure 5. Various modes of depicting the Riemann surface $\Sigma_x = \{t = \mathsf{Re}(\sqrt{z})\}$ of the multi-valued function $z^{\{1/2\}}$. The surface resides in the real 3D-space $\mathbf{C}^1{}_z \times \mathbf{R}^1{}_t$.

In the case of ~~a~~ circular cylinder, we show (diagram (c)) only the intersection Q of Σ_x with the surface H of the cylinder. Cutting H along a vertical line opens H into a rectangle. The rectangle retains the intersection pattern Q. This pattern is especially informative when we are trying to count the number of loops in the boundary of the portion of Σ that is contained in the subset $\{(z, w): |z| \leq r\}$ of the space $\mathbf{C}^2{}_{zw}$. As you see, the intersection of Σ_x with the surface of the cylinder $\{(z, t): |z| \leq r\}$ forms a single self-intersecting loop.

It is clear from Fig. 5 that the behaviour of the projection $\pi: \Sigma_x \to \mathbf{C}^1{}_z$ over the origin 0 is qualitatively different from its behaviour over any other point z in $\mathbf{C}^1{}_z$. Such special point (like the origin) in the target space is called a *ramification point* of the map π. The subset $F_z = \pi^{-1}(z)$ of Σ is called the *fiber* of the map π over the point z.

In fact, Riemann surfaces do not solve all our problems with multi-valued formulas in a single complex variable: for example, there is no simple connection between the Riemann surfaces of the multi-valued functions $f(z) = \sqrt[3]{z}$, $g(z) = \sqrt{1+z}$ and their sum $h(z) = \sqrt[3]{z} + \sqrt{1+z}$. The first one, Σ^f, is the cubic parabola $\{w^3 = z\}$; the second one, Σ^g, is the quadratic parabola $\{w^2 = z + 1\}$; the third one, Σ^h, is an algebraic curve of degree 6 whose equation $\{(w^3 + 3zw + 3w - z)^2 = (1 + z)(3w^2 + z + 1)^2\}$ we did not bother to simplify.
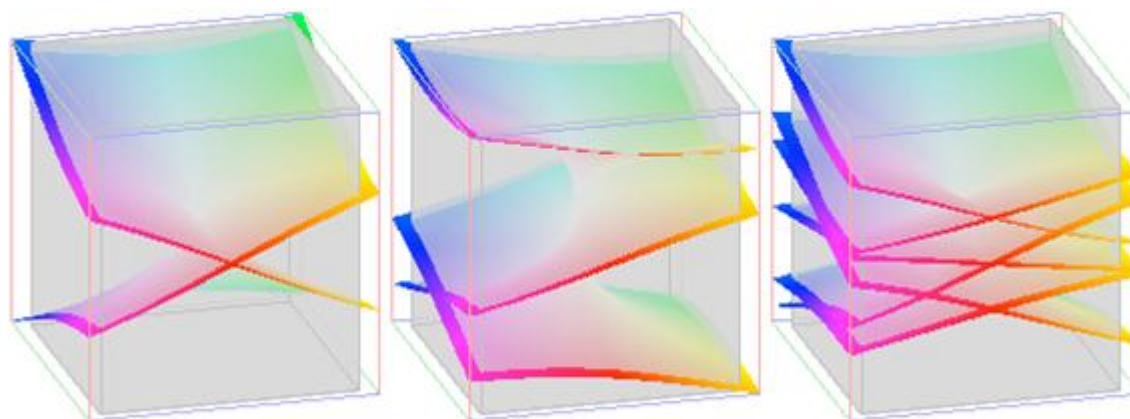
Figure 6. The Riemann surfaces of $\sqrt[3]{z}$, $\sqrt{1+z}$, and $\sqrt[3]{z} + \sqrt{1+z}$.

The three surfaces Σ^f, Σ^g, and Σ^h, are not related in any obvious way (see Fig. 6 which shows the surfaces Σ^f_x, Σ^g_x, and Σ^h_x,), except for the evident relation between their ramification points. However, they testify that, for each z in $\mathbf{C}^1_z$, there is a peculiar way of *continuous coupling* of elements from the fiber Σ^f_z (of cardinality ≤ 3) with the elements of the Σ^g_z (of cardinality ≤ 2), so that the coupling produces elements of the fiber Σ^h_z (of cardinality ≤ 6)! Note that there are exactly 6 handshakes between the members of a group of two friends and the members of a group of three friends…

Our hope is that creating graphical representations like Fig. 5 and Fig. 6 will help students to develop intuitive mental models of the ramification phenomenon, pivotal for the theory of multivalued complex functions.

Investigating the Quadratic Formula with *VisuMatica*

After getting somewhat familiar with the notion of a Riemann surface and the geometry of multi-valued functions it reflects, let us revisit the familiar quadratic formula - $\frac{p}{2} + \sqrt{\frac{p^2}{4} - q}$. Each of its two values satisfies the equation $w^2 + pw + q = 0$. We can study the surface S whose equation in the *pqw*-space (real or complex) is $\{w^2 + pw + q = 0\}$ (see Fig. 7). The surface S is equipped with the projection $\pi: S \to \mathbf{R}^2_{pq}$ (or $\pi: S \to \mathbf{C}^2_{pq}$), where $\pi(p, q, w) = (p, q)$, and with the coordinate function $w: S \to \mathbf{R}$ (or $w: S \to \mathbf{C}$). The construction of S resembles a high-dimensional analogue of the Riemann surface construction: one replaces the multi-valued formula $f(p, q) = -\frac{p}{2} + \sqrt{\frac{p^2}{4} - q}$ with the "honest" function $w: S \to \mathbf{C}$.

Our graphics ability to show the projection of S onto $\mathbf{C}^2_{pq}$ is even more limited than our ability to portray Riemann surfaces. Nevertheless, since *VisuMatica* does a decent job of

showing Riemann surfaces in 3D, we take advantage of this ability to get insights into the geometry of projection $\pi\colon S \to \mathbf{C}^2_{pq}$.

Let us pick a complex line or a curve C in the pq-coefficient space. Consider the complex curve $\Sigma = \pi^{-1}(C)$, the "slice" Σ of S suspended over C. Then we have a chance to visualize the projection $\pi\colon \Sigma \to C$.

For example, take the line $\{p = const\}$ for the role of C. In particular, the q-axis $\{p = 0\}$ is a good example to start with. Then the quadratic formula collapses to $f(0, q) = \sqrt{-q}$, and in the q-direction we see a copy of the familiar Riemann surface for the radical $\sqrt{z}$. The behaviour of $\pi\colon \Sigma \to C$, where C is a line transversal to the *discriminant curve* $D = \{p^2/4 - q = 0\}$ at a point (p, q), is similar.

For a generic line C, the map $\pi\colon \Sigma \to C$ has two ramification points; these are the points where the line C hits the discriminant curve D. Fig. 7 shows the lift to Σ of a loop γ in C that captures: a) none of the ramification points (then $\pi^{-1}(\gamma)$ consists of two loops and π is 1-to-1 on each of them), b) a single ramification point (then $\pi^{-1}(\gamma)$ consists of a single loop and π is 2-to-1 on it), c) both ramification points (again, $\pi^{-1}(\gamma)$ consists of two loops and π is 1-to-1 on each of them). In Fig. 7, we have chosen the line $\{q = 1+ i\}$ for the role of C.

In fact, outside *VisuMatica,* we do not know about any attempts to visualize the geometry of complex quadratic formula.

Visualizing the Cardano Cubic Formula and its S_3-symmetry

In a similar spirit, let us investigate the solutions of depressed *cubic* equations $z^3 + pz + q = 0$.

The substitution $z = w - 3p/w$ transforms this equation into an auxiliary equation $w^6 + qw^3 - p^3/27 = 0$ of degree six. The latter admits solutions in radicals. In fact, its general solution w is given by the formula $\alpha(p, q) = [-q/2 + (q^2/4 + p^3/27)^{\{1/2\}}]^{\{1/3\}}$, a 6-valued function in the complex variables p, q. Moreover, any solution z of the original cubic equation is given by the Cardano Formula $\alpha(p, q) - 3p/\alpha(p, q)$ (see [2]).

Let us explore the geometry and symmetry of the Cardano formula with *VisuMatica*.

Fig. 8 shows a remarkably symmetric pattern of values $\{\alpha(p, q)\}$, where $q = Ap + B$. Note that the six values of α split into two triples, each of which forms a *regular* triangle. The two triangles can be exchanged by a rational linear transformation of the complex plane, a transformation which resembles the inversion map with respect to a given circle. In fact, the action of $\mathbf{S}_3$, the permutation group in tree elements, preserves the configuration of six points in Fig. 8.

It is interesting to observe that the three solutions of the original cubic equation $z^3 + pz + q = 0$ do not exhibit any evident symmetry. In a sense, it is the hidden $\mathbf{S_3}$-symmetry of the auxiliary equation that allows for the solution of the original cubic equation in radicals!
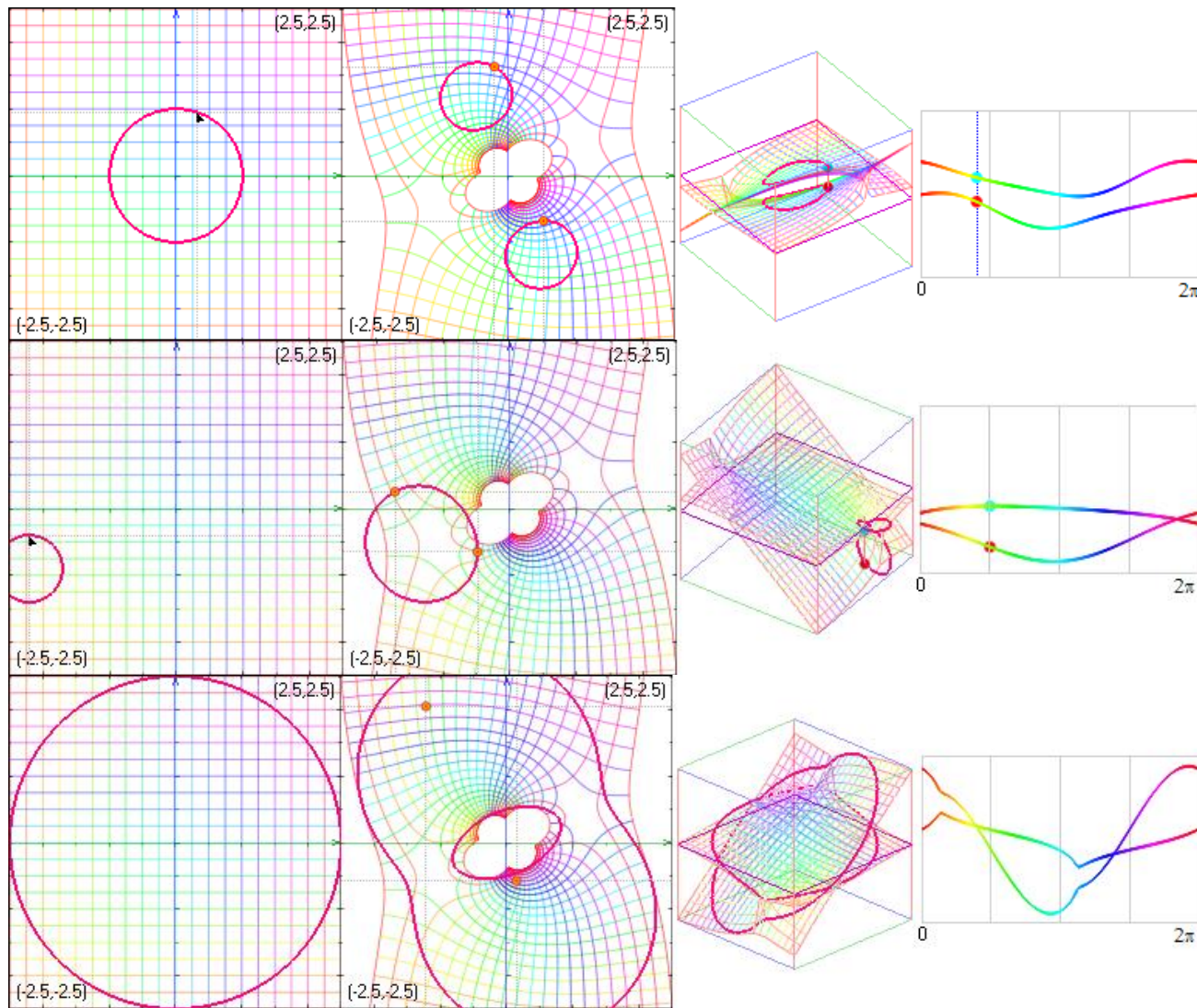

Figure 7. Lifting to the surface Σ different loops γ in the plane (complex line) C. The loops γ capture in distinct ways some ramification points of the map $\pi\colon \Sigma \to C$.

Let us take these observations further.

Denote by $\mathbf{S}$ the surface $\{z^3 + pz + q = 0\}$ in and by $\mathbf{W}$ the surface $\{w^6 + qw^3 - p^3/27 = 0\}$. Both surfaces project on the coefficient plane $\mathbf{C}^2_{pq}$. Moreover, the substitution $z = w - 3p/w$ gives rise to a partially defined 2-to-1 ramified map $k\colon \mathbf{W} \to \mathbf{S}$.
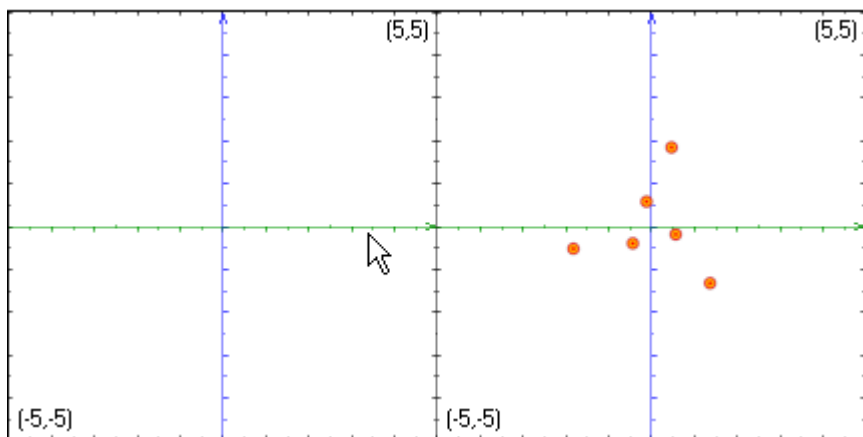
Figure 8. The $\mathbf{S}_3$-symmetrical pattern of the set $\alpha(p, Ap + B)$

As in case with the quadratic formula, we will visualize complex *slices S* and *W* of $\mathbf{S}$ and $\mathbf{W}$ that are suspended over a typical line C in $\mathbf{C}^2{}_{pq}$. Fig. 10 (cf. Fig. 3) shows the Riemann surface of the complex function $\alpha(p, p - i)$. Fig. 11 depicts the nature of the map $\pi: W \rightarrow C$ in the vicinity of its ramification points. For generic line C, they are the three points where C hits the complex *discriminant curve* $D = \{q^2/4 + p^3/27 = 0\}$ (see Fig. 9 for the real analogue of the curve D) and a singleton where C hits the coordinate line $\{p = 0\}$. These pictures help us to reconstruct the topology of a typical slice W, shown in Fig. 12 (see [6], [7] for more details). It exhibits a remarkable $\mathbf{S}_3$-symmetry, where $\mathbf{S}_3$ denotes the permutation group in 3 symbols.
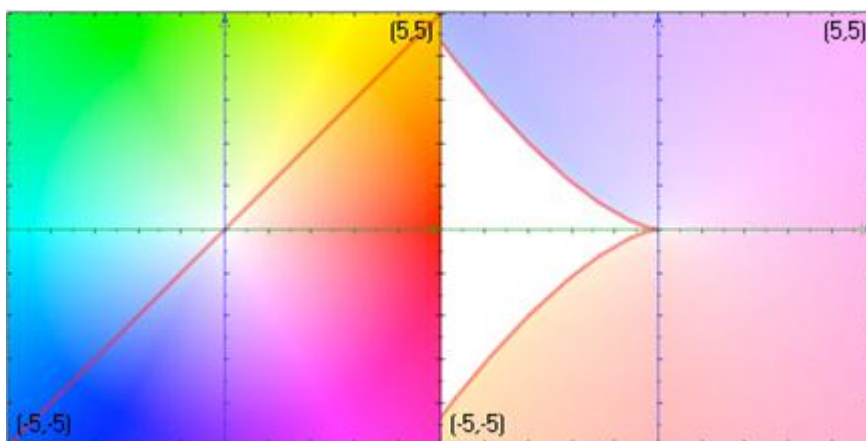

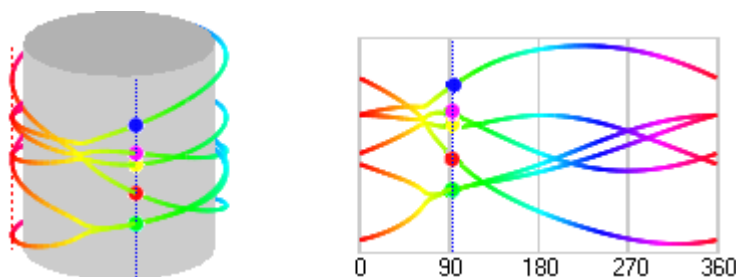Figure 9. The real discriminant curve $D = \{q^2/4 + p^3/27 = 0\}$

Figure 10. The Riemann surface of the Cardano function $\alpha(p, p - i)$ over the circle $|p|=1.25$
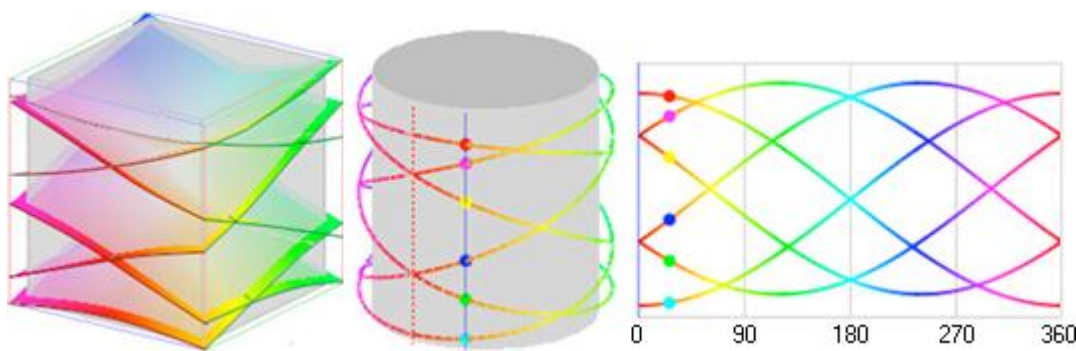

Figure 11. The Riemann surface $\pi: W \to L$ over a big square/disk U in the complex line L. Note that $\pi^{-1}(\partial U)$ consists of 3 loops.

Fig. 11 and its variations help to analyse the topology of the slice W of the surface $\mathbf{W} = \{w^6 + qw^3 - p^3/27 = 0\}$ over a generic line L in the coefficient plane $\mathbf{C}^2_{pq}$. The next Fig. 12 depicts the ecstatically pleasing results of this analysis.

Of course, an algebraic geometer will easily determine this topology using some standard computational techniques ([2], [8]). Again, our point is that VisuMatica can replace these relatively advanced computations with dynamic interactive models that faithfully reflect them.

Note the complex curve W has two singularities one of which resides "at ∞". Each of the two singular points, 0 and ∞, has a small neighbourhood in W whose the boundary consist of 3 loops (Fig. 11 shows these three loops in the vicinity of ∞, and Fig. 12 delivers a "global view" of W and its singularities).

Figure 12. The topology of a typical slice W of the Cardano surface $\mathbf{W}$ over a generic line L in $\mathbf{C}^2_{pq}$.

Visualizing the Monodromy of Riemann Surfaces while Exploring the Abel-Ruffini Theorem

In studying the solvability of polynomial equations $P(z) = 0$, it is important to understand the so called *monodromies* of the Riemann surface Σ_P associated with a given equation. As usual, we call *VisuMatica* for help.

In this context, monodromies are transformations of the fibers $\pi^{-1}(p)$ of map $\pi\colon \Sigma_P \to \mathbf{C}$, the transformations that occur as p traces a loop in $\mathbf{C}$. The right diagrams in Figures 10 and 11 will give the reader an intuitive feel for the monodromy concept: just follow each curve on the surface of cylinders to see where it starts and ends on a fixed vertical line.

We will not attempt here to explain the Geometric Galois Theory (see [1], [6]) in its full generality. Instead, consider one specific p-family of equations: $\{z^5 - z + p = 0\}$.

The famous Abel-Ruffini Theorem claims that the equations $\{z^5 - z + p = 0\}$ *have no solutions in radicals* for all, but finitely many values of p!

Let Σ be the curve $\{z^5 - z + p = 0\}$ in $\mathbf{C}^2_{pz}$ equipped with the projection $\pi\colon (z, p) \to p$ on the p-coordinate line $\mathbf{C}$. This map $\pi\colon \Sigma \to \mathbf{C}$ is ramified over four points p_1, p_2, p_3, p_4 in $\mathbf{C}$. As we trace a loop γ in the complement Π to these four points, at each point p of γ, a *permutation* of the fiber $\pi^{-1}(p)$ is generated (note that $\pi^{-1}(p)$ is exactly the set of all five roots of the equation $z^5 - z + p = 0$). This permutation is an element of $\mathbf{S}_5$, the permutation group in five elements (see Fig. 12).

An important step in proving the Abel-Ruffini Theorem is to check that any permutation from $\mathbf{S}_5$ can be realized as the monodromy of $\pi\colon \Sigma \to \mathbf{C}$ along an appropriate loop γ in Π (an algebraist would say: "$\mathbf{S}_5$ is the Galois group of a generic equation $z^5 - z + p = 0$"). Eventually, this conclusion clashes with the assumption that there exists a formula in radicals that solves all equations of the form $z^5 - z + p = 0$.
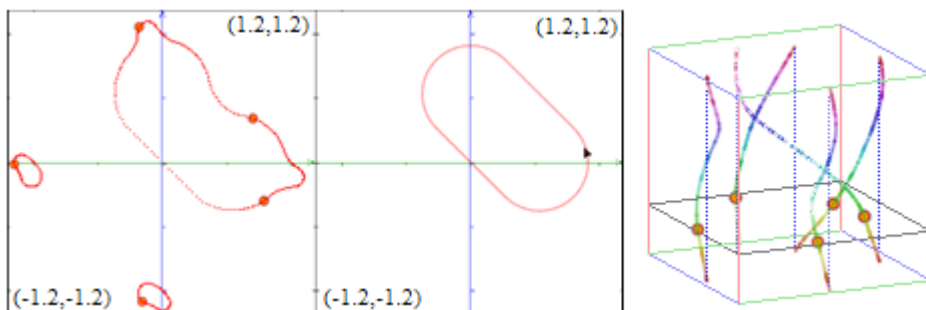

Figure 13. The cyclic permutation of order 3 of the fiber $\pi^{-1}(p)$ of the ramified map $\pi\colon \Sigma \to \mathbf{C}$. The permutation is induced by moving along the loop γ (the oval on the right), which encapsulates only two ramification points of π.

The RHS diagram in Fig. 12 provides us with an effective visualisation of the monodromy of the map $\pi\colon \Sigma \to \mathbf{C}$. This pattern of five strings is called a *braid*. The braids can be interpreted as elements of a group $\mathbf{B}_5$, an extension of the permutation group $\mathbf{S}_5$. Braid groups play an important role in algebra, topology, and the singularity theory. So *VisuMatica* is able to portray braids well.

Concluding remarks

[6] and [1] contain a variety of projects and virtual experiments that extend the ones suggested by this paper, as well as an explanation of mathematical theory behind them. Although such theory resides on the border between undergraduate and graduate mathematics, the interactive use of *VisuMatica* makes it much more accessible to students with different mathematical backgrounds.

References

[1] Alekseev, V.B., Abel's Theorem in Problems and Solutions, Moscow State University, Moscow (1976).

[2] Brieskorn, E., Knorrer, H., Plane Algebraic Curves, Birkhauser Verlag, Basel-Boston-Stuttgart (1986).

[3] http://cinderella.de/tiki-index.php

[4] Farris, F., Visualizing complex-valued functions in the plane. MAA online, http://www.maa.org/pubs/amm_complements/complex.html

[5] http://www.dynamicgeometry.com/

[6] Katz, G., Nodelman, V., The Shape of Algebra in the Mirrors of Mathematics, World Scientific Publishing (2011).

[7] Katz, G., Nodelman, V., Computer-aided explorations of modular spaces of real polynomials: Giving geometric life to routine algebra The Electronic J. of Mathematics and Technology 5(1), 2011.

[8] Kirwan, F., Complex Algebraic Curves, London Mathematical Society, Cambridge University Press (1992).

[9] Nodelman, V., Multiple Views in Educational Software for Mathematics. Proc. The 2006 World Congress in Computer Science Computer Engineering, and Applied Computing - MSV'06. The 2006 Int'l. Conf.on Modeling, Simulation and Visualization Methods. Las Vegas, Nevada, USA, 26-29 June 2006 (210-213).

[10] Thaller, B., Visualization of Complex Functions. The Mathematica® Journal http://www.mathematica-journal.com/issue/v7i2/articles/contents/thaller/html/

[11] Wagon, S., Mathematica in Action. Problem Solving Through Visualization and Computation. 3ed, Springer (2010).

[12] Wegert, E., Visualization of Complex Functions. Plea for the Phase Plot (2009).